

# AMS02 results support the secondary origin of cosmic ray positrons

Kfir Blum,<sup>1,\*</sup> Boaz Katz,<sup>1,2,†</sup> and Eli Waxman<sup>3,‡</sup>

<sup>1</sup>*Institute for Advanced Study, Princeton 08540, USA*

<sup>2</sup>*Bahcall Fellow*

<sup>3</sup>*Dept. of Part. Phys. & Astrophys., Weizmann Institute of Science, POB 26, Rehovot, Israel*

We show that the recent AMS02 positron fraction measurement is consistent with a secondary origin for positrons, and does not require additional primary sources such as pulsars or dark matter. The measured positron fraction at high energy saturates the previously predicted upper bound for secondary production [1], obtained by neglecting radiative losses. This coincidence, which will be further tested by upcoming AMS02 data at higher energy, is a compelling indication for a secondary source. Within the secondary model the AMS02 data imply a cosmic ray propagation time in the Galaxy of  $< 10^6$  yr and an average traversed interstellar matter density of  $\sim 1 \text{ cm}^{-3}$ , comparable to the density of the Milky Way gaseous disk, at a rigidity of 300 GV.

**Introduction.** The AMS02 experiment announced a new measurement of the positron fraction (ratio of  $e^+$  to total  $e^\pm$  flux) in Galactic cosmic rays (CRs) [2]. The new measurement extends to high energy,  $E \sim 350$  GeV, with precision significantly superseding earlier experiments [3–5]. The positron fraction is found to increase with energy, apparently saturating at  $e^+/e^\pm \sim 0.15$  at  $E \sim 200$  GeV.

A rising positron fraction stands in conflict with expectations based on popular diffusion models, assuming a homogeneous diffusion coefficient and a cosmic ray halo scale height that is independent of cosmic ray rigidity. This conflict has triggered numerous analyses invoking hypothetical primary sources for the positrons such as pulsars and annihilation or decay of dark matter particles.

In this paper we point out that the AMS02 measurement [2] is in fact consistent with the simplest possible estimate due to the one guaranteed  $e^+$  source: the secondary production of  $e^+$  by the collision of high energy primary CRs with ambient interstellar matter (ISM). The main result of this paper is contained in Fig. 1. There, AMS02  $e^+/e^\pm$  data (black) at high energy is seen to coincide with an upper bound for secondary production (green, cyan uncertainty band), previously derived in [1] by ignoring the radiative losses of the positrons.

In the rest of this paper we outline the derivation of Fig. 1, explaining why the AMS02 result provides a strong hint for a secondary positron source. We comment on the implications of a rising positron fraction, that is not in conflict with a secondary source. Assuming secondary production, we then highlight the constraints imposed by the new measurement on models of CR propagation in the Galaxy.

**AMS02 and the secondary positron flux.** While the propagation of CRs in the galaxy is poorly understood, the expected fluxes of secondaries, such as positrons, are tightly constrained by the measurement of other secondaries, such as boron. This results from the fact that (i) different relativistic particles with the same

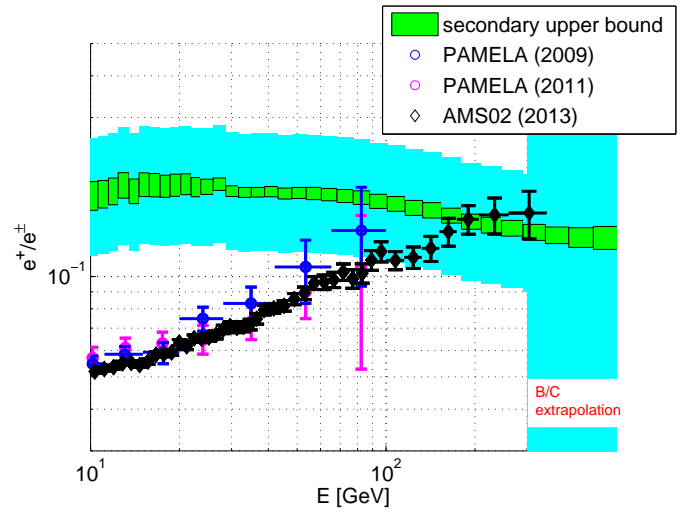


FIG. 1: Positron flux upper bound vs. data. Green shows the  $e^+$  upper bound prediction of Ref. [1], divided by the  $e^\pm$  flux measured by FERMI [6]; bin widths correspond to the FERMI  $e^\pm$  measurement uncertainties. Cyan shows an estimated calculation uncertainty on the  $e^+$  flux upper bound. AMS02 [2], early [3] and subsequent [4] PAMELA data are shown in black, blue and magenta. Note that extending the calculation to  $E > 300$  GeV (shaded region on the right) involves an extrapolation of B/C data; see text.

rigidity (momentum divided by charge) propagate in a magnetic field in the same way, regardless of the magnetic field configuration; and (ii) the production rates of all secondaries are correlated in a calculable manner.

The measured number densities  $n_i$  of stable secondary CR nuclei are proportional to their net local production rate and are thus well described by

$$n_i = \frac{X_{\text{esc}} \sum_{j>i} n_j (\sigma_{j \rightarrow i} / m_p)}{1 + (\sigma_i / m_p) X_{\text{esc}}}, \quad (1)$$

where  $\sigma_{j \rightarrow i}$  is the decayed spallation cross section of the parent nucleus  $j$  into the secondary  $i$  per ISM nucleon

and  $\sigma_i$  is the cross section for destruction of  $i$  per ISM nucleon. The grammage  $X_{\text{esc}}$ , defined by Eq. (1), parameterizes the column density of target material traversed by the CRs and is the same for all species. The value of  $X_{\text{esc}}$  is measured to be

$$X_{\text{esc}} = 8.7 \left( \frac{E/Z}{10 \text{ GeV}} \right)^{-0.5} \text{ g cm}^{-2}, \quad (2)$$

with different fits varying by  $\sim 30\%$  in the range  $10 \text{ GeV} < E/Z \lesssim 100 \text{ GeV}$  [7–10].

Eq. (1) does not capture the effect of energy loss during propagation. This means that it cannot be directly applied to positrons, since they are subject to Synchrotron and inverse-Compton (IC) losses. Nevertheless, it was realized in [1] that Eq. (1) provides a robust upper limit to the positron flux, given that radiative losses can only decrease the flux of the steep positron spectrum. This upper limit is model independent, derived from data and requires no free parameters.

Positron fraction measurements by AMS02 [2] and PAMELA [3, 4] are compared to the upper bound of Eq. (1) in Fig. 1. Since the experiments did not report the positron flux, but only the  $e^+/e^\pm$  fraction, we present the upper bound by dividing the theoretical  $e^+$  flux by the total  $e^\pm$  FERMI flux measurement [6]. As demonstrated in the figure, the upper limit is not violated by the new AMS02 data. This means that the data is consistent with secondary positrons. Moreover, at high energy the measured positron fraction saturates within the secondary limit, previously predicted in [1]. This coincidence, while yet to be further tested by future AMS02 data at higher energy, is a compelling hint for a secondary source.

It is worthwhile to compare this result to models invoking new primary sources such as pulsars or dark matter. In such models, ad-hoc tuning of free parameters is required to account for the positron fraction saturating at  $\sim 0.15$  for  $E \gtrsim 200 \text{ GeV}$ . The distinction between the secondary and primary models is even more transparent when considering the absolute  $e^+$  flux. In contrast to the  $e^+/e^\pm$  fraction, that has a limited dynamical range, the  $e^+$  flux due to primary sources could well have been orders of magnitude below or above the secondary bound. We know of no intrinsic scale, and thus of no reason, in any of the primary injection models suggested in the literature, for the positron flux to lie close to the data-driven secondary bound, throughout the range  $E \sim 10 - 300 \text{ GeV}$ .

**A  $\bar{p}$  consistency check, future tests of the secondary model, and calculation uncertainties.** A test of the validity of our calculations is presented in Fig. 2, where the measured flux of secondary antiprotons [11], that are produced in the same interactions as secondary positrons, is compared to the flux obtained from Eq. (1). As seen in the figure, our calculation is consistent with the observations.

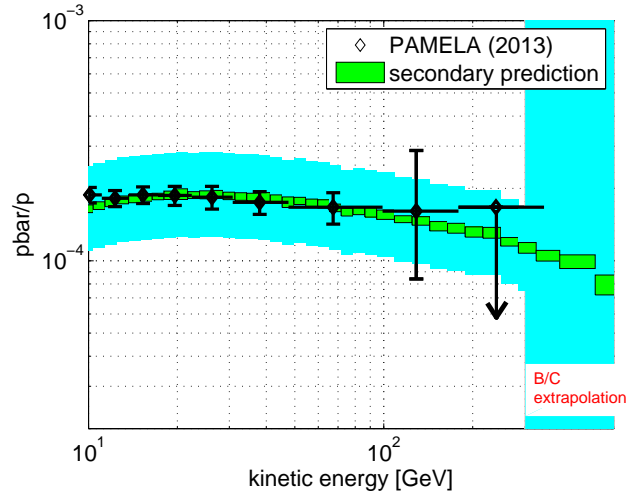


FIG. 2: PAMELA  $\bar{p}/p$  data [11] vs. the secondary source prediction of Eq. (1). Cyan shows an estimated calculation uncertainty on the secondary prediction. Note that extending the calculation to  $E > 300 \text{ GeV}$  (shaded region on the right) involves an extrapolation of B/C data; see text.

The secondary source hypothesis will be further tested with upcoming AMS02 measurements of the  $e^+$  and  $\bar{p}$  flux at higher energy, up to the TeV range [12]. A potentially useful independent check, though complicated by systematic uncertainties, can be done by analyzing the elemental ratios of nuclei having a radioactive isotope component with a rest frame lifetime of the order of 1 Myr, including Be/B, Cl/Ar and Al/Mg at high rigidity similar to the cooling time of the positrons [1, 13, 14]. A more straightforward check, limited however to  $E/Z \lesssim 10 \text{ GeV}$ , will come from directly measuring the isotopic ratio  $^{10}\text{Be}/^9\text{Be}$ .

We now comment on the systematic uncertainties involved in computing the  $e^+$  upper bound and the  $\bar{p}$  flux. First, we caution that extending the  $e^+$  and  $\bar{p}$  calculations to high energies above 300 GeV, as in Figs. 1 and 2, involves extrapolation. Figs. 1 and 2 were computed using the CR grammage of Eq. (2), extracted from analyses of HEAO3 data and tested only up to  $E/Z \sim 300 \text{ GeV}$  [7]. While there are some indications that the same parametrization of  $X_{\text{esc}}$  may hold to  $E/Z \sim \text{TeV}$  [15], the case is not settled with hints of spectral hardening reported in [16, 17]. Note that a hardening in  $X_{\text{esc}}$  should lead to hardening of all secondaries including  $e^+$  and  $\bar{p}$ . We shade in cyan the rigidity range in Figs. 1 and 2, where Eq. (2) is being extrapolated beyond the current determination of  $X_{\text{esc}}$ . A robust secondary prediction in this range will be possible with improved boron/carbon (B/C) measurements, expected from AMS02 [12].

Additional systematic uncertainties, estimated roughly by 50% for both the  $e^+$  and  $\bar{p}$  calculations, are denoted

by the cyan bands in Figs. 1 and 2. The main potential sources of error are these:

(i) *Different cross section parameterizations* for hadron production in  $pp$  and  $pA$  collisions, differ by energy-dependent factors in the order of tens of percent. The difficulty is the inapplicability of perturbative calculations, together with the scarcity of accelerator data for soft charged hadron production, particularly at high rapidity. Resolving this ambiguity is beyond the scope of the current paper. Here we follow the same calculation done in [1], to which we refer the reader for more details.

(ii) *We expect Eq. (1) to only apply to  $\approx 10\%$  accuracy*, which is roughly the level at which the assumption of negligible energy change during propagation can be expected to hold for stable secondary nuclei. We also estimate about 30% uncertainty for  $X_{\text{esc}}$  at 100-300 GeV/nuc.

(iii) *The primary CR nuclei flux and composition* at the 0.1-10 TeV/nuc range, responsible for  $\sim 10$ –100 GeV  $e^+$  and  $\bar{p}$  production, are still somewhat uncertain [18]. Existing measurements at the relevant range [19–21] differ systematically by 20-30%. In our analysis we adopt a proton flux interpolating the published PAMELA data [19] below a TeV and the CREAM data [21] up to  $E = 100$  TeV.

Finally, we comment that the combination of AMS02  $e^+/e^\pm$ , FERMI  $e^\pm$ , and PAMELA  $p$  and He measurements, required here in order to compare the secondary predictions to data, is prone to systematic errors. It would be preferable to use direct measurements of all of these ingredients by AMS02.

**On a positron fraction rising with energy.** Due to synchrotron and IC energy losses, the positron flux is suppressed, compared to the upper bound, by an energy dependent factor  $f_{e^+} < 1$ .  $f_{e^+}$  should increase monotonically as a function of  $t_{\text{cool}}/t_{\text{esc}}$ , where  $t_{\text{cool}}$  is the  $e^+$  radiative cooling time and  $t_{\text{esc}}$  is the mean propagation time. In the limit  $t_{\text{cool}}/t_{\text{esc}} \gg 1$ , we expect  $f_{e^+} \rightarrow 1$ .

The claims in the literature, that the increase with energy of the positron fraction is inconsistent with a secondary origin, are based on two lines of reasoning, neither of which is supported by data (see [1] for a detailed discussion). The first line of reasoning assumes that (i) primary  $p$  and  $e^-$  have the same production spectrum, and (ii) primary  $e^-$  and secondary  $e^+$  suffer the same energy losses. Both (i) and (ii) are unsubstantiated. It is plausible that primary  $e^-$  suffer additional energy loss at the primary CR sources and that the injected  $e^-$  spectrum is different than that of the protons. The second line of reasoning adopts some specific propagation model, which leads to  $t_{\text{cool}}/t_{\text{esc}}$  (and so to  $f_{e^+}$ ) that decreases with energy. Such behavior of  $t_{\text{cool}}/t_{\text{esc}}$  and  $f_{e^+}$  can be modified in alternative models.

This discussion makes clear that given the current AMS02 data, depicted in Fig. 1, the call for primary sources is unconvincing. Since both  $t_{\text{cool}}$  and  $t_{\text{esc}}$  are neither directly measured nor reliably calculable, the en-

ergy dependence of  $f_{e^+}$ , and hence of the positron fraction, can not be reliably predicted. The positron data should be regarded as a first direct measurement of  $f_{e^+}$ , with interesting implications for the times scales  $t_{\text{esc}}$  and  $t_{\text{cool}}$  (see e.g. [22, 23], and more recently [1, 14]).

### Interpretation: constraints on CR propagation.

In the rest of this paper we assume that the positron flux is of secondary origin, and proceed to deduce new constraints on CR propagation.

The secondary model allows us to quantify the amount by which the positron flux is suppressed by propagation energy loss, based on the observations. The suppression factor  $f_{e^+}$  is given by the ratio between the observed  $e^+$  flux to the calculated upper bound. This corresponds, in Fig. 1, to the ratio of the black data to the green curve. We now analyze the constraints arising from Fig. 1.

1. *CR propagation time.* If we ignore Klein-Nishina corrections (see discussion below), then Fig. 1 implies that:

$$t_{\text{esc}}(E/Z = 200 \text{ GeV}) \leq t_{\text{cool}}(E = 200 \text{ GeV}) \\ \sim 1.7 \text{ Myr} \left( \frac{\bar{U}_T}{1 \text{ eVcm}^{-3}} \right)^{-1}, \quad (3)$$

$$t_{\text{esc}}(E/Z = 10 \text{ GeV}) > t_{\text{cool}}(E = 10 \text{ GeV}) \\ \sim 30 \text{ Myr} \left( \frac{\bar{U}_T}{1 \text{ eVcm}^{-3}} \right)^{-1}. \quad (4)$$

Here  $\bar{U}_T$  is the time-averaged total electromagnetic energy density in the propagation region. Note that it is natural to expect that  $\bar{U}_T$  should depend on CR rigidity. Thus  $\bar{U}_T$  should be understood as function of  $E$ , though we omit the explicit dependence for clarity of notation.

One irreducible source for energy dependence in the effective value of  $\bar{U}_T$  comes from Klein-Nishina corrections, that are neglected in Eqs. (3) and (4) which were derived in the Thomson limit. The Thomson limit is not a good approximation for 20-200 GeV positrons if  $\bar{U}_T$  contains a significant UV component, as appears to be the case from estimates of the Milky Way radiation field [24]. In that case, the effective radiation energy density for an  $\sim 200$  GeV  $e^+$  can be significantly lower than that for an  $\sim 10$  GeV one (see e.g. [25]). In Fig. 3 we plot the cooling time  $t_{\text{cool}}$  for electrons and positrons under different assumptions for  $\bar{U}_T$ . Smooth lines set the UV component to zero. Dashed lines show varying amounts of UV light having a black body spectrum with a temperature  $T = 6000$  K.

2. *The mean ISM density of the CR halo.* We can now estimate the mean ISM density traversed by CRs. Using Eq. (2) together with Eqs. (3) and (4), we find

$$\bar{n}_{\text{ISM}}(E/Z = 200 \text{ GeV}) \gtrsim 0.6 \left( \frac{\bar{U}_T}{1 \text{ eVcm}^{-3}} \right) \text{ cm}^{-3}, \quad (5)$$

$$\bar{n}_{\text{ISM}}(E/Z = 10 \text{ GeV}) \lesssim 0.15 \left( \frac{\bar{U}_T}{1 \text{ eVcm}^{-3}} \right) \text{ cm}^{-3}, \quad (6)$$

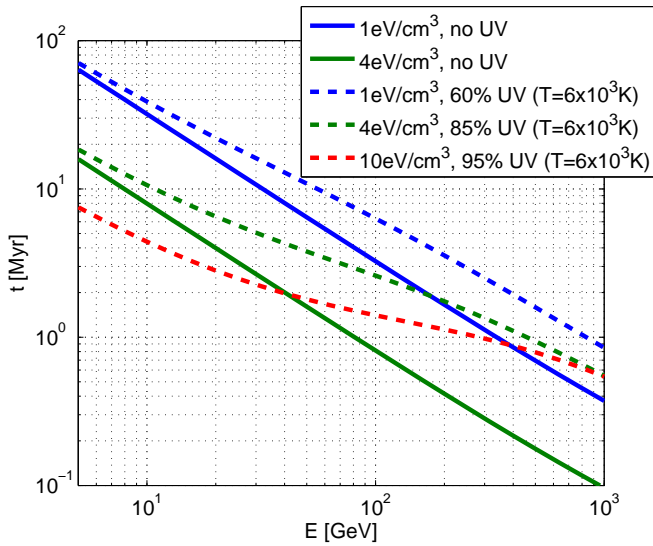


FIG. 3: Cooling time  $t_c$  for  $e^\pm$  radiative losses, as function of  $e^\pm$  energy, for different assumptions regarding the total electromagnetic energy density and its UV component.

assuming an ISM composition of 90% $H$ +10% $He$  by number.

Eqs. (5) and (6) suggest that the confinement volume of CRs decreases with increasing CR rigidity, to the extent that CRs at  $E/Z \sim 200$  GeV spend much of their propagation time within the thin Galactic HI disc, with a scale height  $h \simeq 200$  pc, while CRs at  $E/Z \sim 10$  GeV probe a larger halo. These are not robust conclusions, however. For example, if a significant fraction of the grammage  $X_{\text{esc}}$  is accumulated during a short time in relatively dense regions, e.g. near the CR source, then the halo could be larger. Significant energy dependence in  $\bar{U}_T$  could further affect the interpretation. For example,  $\bar{U}_T \propto E^{-0.5}$  (inspired by the CR grammage  $X_{\text{esc}} \propto E^{-0.5}$ ) would allow for a rigidity independent  $\bar{n}_{\text{ISM}}$ .

**Conclusions.** The positron fraction measured recently by AMS02 is consistent with the upper bound predicted in Ref. [1], assuming a secondary source. Upcoming AMS02 measurements of the  $e^+$  and  $\bar{p}$  flux at yet higher energies will continue to test the model.

At the highest measurement energy, the positron flux saturates the upper bound, and throughout the measurement range it is never smaller than a factor of  $f_{e^+} \sim 0.3$  compared to it. We find this to be a compelling hint for a secondary source. Considering hypothetical primary sources such as pulsars or dark matter, we know of no intrinsic scale in these models that would fix the positron flux at this particular range.

Interpreted under the secondary source hypothesis, the positron data places interesting constraints on the propagation time of CRs at  $E/Z \sim 10 - 300$  GeV,

that we roughly summarize by  $t_{\text{esc}}(10 \text{ GeV}) \gtrsim 30 \text{ Myr}$  and  $t_{\text{esc}}(200 \text{ GeV}) \lesssim \text{Myr}$ . The constraint on  $t_{\text{esc}}$  at  $E/Z > 100$  GeV is obtained by the new positron data, with no direct counterpart in earlier CR data. The constraint at  $E/Z \sim 10$  GeV is consistent, within uncertainties, with measurements of the elemental ratios of radioisotopes [1, 13, 14].

Using the measured CR grammage together with the new constraints on  $t_{\text{esc}}$ , we derive the mean ISM particle density in the propagation region of high energy CRs,  $\bar{n}_{\text{ISM}} > 0.6 \text{ cm}^{-3}$  for  $E/Z = 200$  GeV. This result for  $\bar{n}_{\text{ISM}}$  is comparable to the mean ISM density in the Milky Way HI disc. At  $E/Z = 10$  GeV we find a smaller mean density,  $\bar{n}_{\text{ISM}} < 0.15 \text{ cm}^{-3}$ . Put together, these numbers could mean that the scale height of the CR halo decreases with increasing CR rigidity (however, see discussion following Eqs. 5 and 6 for caveats in this interpretation).

**Acknowledgments.** We thank Moti Milgrom, Kohta Murase and Rashid Sunyaev for discussions. KB is supported by DOE grant DE-FG02-90ER40542. BK is supported by NASA through the Einstein Postdoctoral Fellowship awarded by Chandra X-ray Center, which is operated by the Smithsonian Astrophysical Observatory for NASA under contract NAS8-03060. EW is partially supported by GIF and UPBC grants.

\* Electronic address: kblum@ias.edu

† Electronic address: boazka@ias.edu

‡ Electronic address: eli.waxman@weizmann.ac.il

- [1] B. Katz, K. Blum, and E. Waxman, *Mon.Not.Roy.Astron.Soc.* **405**, 1458 (2010), 0907.1686.
- [2] M. Aguilar, G. Alberti, B. Alpat, A. Alvino, G. Ambrosi, K. Andeen, H. Anderhub, L. Arruda, P. Azzarello, A. Bachlechner, et al. (AMS Collaboration), *Phys. Rev. Lett.* **110**, 141102 (2013), URL <http://link.aps.org/doi/10.1103/PhysRevLett.110.141102>.
- [3] O. Adriani et al. (PAMELA Collaboration), *Nature* **458**, 607 (2009), 0810.4995.
- [4] O. Adriani, G. Barbarino, G. Bazilevskaya, R. Bellotti, M. Boezio, et al., *Astropart.Phys.* **34**, 1 (2010), 1001.3522.
- [5] M. Ackermann et al. (Fermi LAT Collaboration), *Phys.Rev.Lett.* **108**, 011103 (2012), 1109.0521.
- [6] M. Ackermann et al. (Fermi LAT Collaboration), *Phys.Rev.* **D82**, 092004 (2010), 1008.3999.
- [7] W. R. Binns, T. L. Garrard, M. H. Israel, M. D. Jones, M. P. Kamionkowski, J. Klarmann, E. C. Stone, and C. J. Waddington, *Astrophys. J.* **324**, 1106 (1988).
- [8] J. Engelmann, P. Ferrando, A. Soutoul, P. Goret, and E. Juliusson, *Astron.Astrophys.* **233**, 96 (1990).
- [9] F. C. Jones, A. Lukasiak, V. Ptuskin, and W. Webber, *Astrophys. J.* **547**, 264 (2001), arXiv:astro-ph/0007293.
- [10] W. R. Webber, F. B. McDonald, and A. Lukasiak, *Astrophys. J.* **599**, 582 (2003).
- [11] O. Adriani, G. Bazilevskaya, G. Barbarino, R. Bellotti, M. Boezio, et al., *JETP Lett.* **96**, 621 (2013).

- [12] A. KOUNINE, International Journal of Modern Physics E **21**, 1230005 (2012).
- [13] W. R. Webber and A. Soutoul, *Astrophys. J.* **506**, 335 (1998).
- [14] K. Blum, *JCAP* **1111**, 037 (2011), 1010.2836.
- [15] H. S. Ahn, P. S. Allison, M. G. Bagliesi, J. J. Beatty, G. Bigongiari, P. J. Boyle, T. J. Brandt, J. T. Childers, N. B. Conklin, S. Coutu, et al., *Astroparticle Physics* **30**, 133 (2008), 0808.1718.
- [16] V. I. Zatsepin, A. D. Panov, N. V. Sokolskaya, J. H. Adams, H. S. Ahn, G. L. Bashindzhagyan, J. Chang, M. Christl, A. R. Fazely, T. G. Guzik, et al., *Astronomy Letters* **35**, 338 (2009), 0905.0049.
- [17] A. Obermeier, M. Ave, P. Boyle, C. Hoppner, J. Horandel, et al., *Astrophys.J.* **742**, 14 (2011), 1108.4838.
- [18] J. Lavalle, *Mon.Not.Roy.Astron.Soc.* **414**, 985L (2011), 1011.3063.
- [19] O. Adriani, G. C. Barbarino, G. A. Bazilevskaya, R. Bellotti, M. Boezio, E. A. Bogomolov, L. Bonechi, M. Bongi, V. Bonvicini, S. Borisov, et al., *Science* **332**, 69 (2011), 1103.4055.
- [20] A. Panov, J. Adams, J.H., H. Ahn, G. Bashinzhagyan, J. Watts, et al., *Bull.Russ.Acad.Sci.Phys.* **73**, 564 (2009), 1101.3246.
- [21] H. Ahn, P. Allison, M. Bagliesi, J. Beatty, G. Bigongiari, et al., *Astrophys.J.* **714**, L89 (2010), 1004.1123.
- [22] V. Ginzburg and V. Ptuskin, *Rev.Mod.Phys.* **48**, 161 (1976).
- [23] V. Ginzburg, V. Dogiel, V. Berezhinsky, S. Bulanov, and V. Ptuskin (1990).
- [24] T. A. Porter and A. Strong (2005), astro-ph/0507119.
- [25] R. Schlickeiser and J. Ruppel, *New J.Phys.* **12**, 033044 (2010), 0908.2183.